DOI: https://doi.org/10.37434/tpwj2024.05.02

THERMOMECHANICAL PROCESSES IN FRICTION STIR WELDING OF MAGNESIUM ALLOY SHEETS

M.A. Khokhlov[1], O.O. Makhnenko[2], V.A. Kostin[1], A.G. Pokliatskyi[1], Iu.V. Falchenko[1], Yu.A. Khokhlova[1]

[1]E.O. Paton Electric Welding Institute of the NASU
11 Kazymyr Malevych Str., 03150, Kyiv, Ukraine
[2]Kyiv Academic University
36 Acad. Vernadskyi Str., 03142, Kyiv, Ukraine

ABSTRACT

Experimental laboratory equipment for friction stir welding (FSW) as a result of working out the optimal welding modes at different linear velocities allows producing high-quality butt joints from thin ductile metals. With the development of new mathematical methods for modeling thermodeformational processes, it became possible to analyze the stress-strain state and thermomechanical processes occurring in the FSW joint zone, which is necessary for predicting the operational properties, strength and service life of welded structures made of thin metal. Using mathematical models and finite element analysis, the temperature distributions from the volume heat source at FSW were visualized, and the residual deformations and stresses in the zone of butt-welded joints of thin sheets of magnesium alloys were numerically determined. In the future, it is advisable to determine the effective balance of the linear speed and the rotation speed of the FSW tool to obtain better homogeneity of the weld structure and reduce heat input into the metal during welding.

KEYWORDS: magnesium alloys, friction stir welding, microstructure, modulus of elasticity, temperature distributions, residual stresses, plastic deformations

INTRODUCTION

Magnesium has high specific strength, high rigidity and damping characteristics, absolute biological compatibility that is why it is included into the top ten of innovative future materials for application in structural elements of aerospace engineering, cars, sports equipment, microelectronics, and in surgical implants [1–3]. The ratio of strength to weight of magnesium alloy parts makes them one of the many important materials, which will replace aluminium and will be used in automotive industry in the coming years to lower the force of inertia and for the benefit of productivity, controllability and fuel saving. A large part of investigations on magnesium alloys weldability considers the experience of application of environmentally-friendly and energy-efficient technology — friction stir welding (FSW) used for solid-phase joining of parts of relatively simple geometry. Statistically successful is the experience [4] of application of a tool in the form of a smooth pin with a concave shoulder at FSW, as it allows avoiding deformation when joining lightweight and ductile alloys; the welds form without cavities and contain locally strengthened zones along the lower contour of the weld nugget [5, 6]. An idea for the subsequent experiments was mathematical modeling of temperature and deformation processes at FSW using fundamental regularities [7–11]. Such a complex approach at evaluation of the quality of welded joint formation is developed for further application in statistical scaled models for prediction of service properties, strength and service life of welded structures from thin magnesium alloys.

The objective of this study is producing sound FSW butt joints of magnesium alloy at a constant speed of the tool rotation and at different linear welding speeds, determination of physical-mechanical parameters of the material in FSW zone by the indentation method, as well as experimental measurement of surface temperature fields at FSW, determination of the temperature fields by mathematical modeling methods, distribution of strains and residual stresses in FSW butt joints.

MATERIALS AND METHODS OF INVESTIGATION

Welding of butt joints of 2 mm sheets of MA2-1 magnesium alloy of Mg–Al–Zn system (Table 1) was performed in experimental welding equipment for FSW

Table 1. Chemical composition of MA2-1 magnesium alloy, wt.%

Fe	Si	Mn	Ni	Al	Cu	Be	Mg	Zn	Others
0.04	0.1	0.3–0.7	0.004	3.8–5.0	0.05	0.002	92.6–95.1	0.8–1.5	0.3

Figure 1. Thermogram of the temperature field at FSW of butt joint of 2 mm magnesium alloy (Fluke Ti25)

at a constant frequency of tool rotation of 1420 rpm and at different linear speeds (8, 16, 24 m/h).

Comparative evaluation of the temperature fields at FSW was performed by experimental infrared thermal imager Fluke Ti25 (Figure 1) and COMSOL Multiphysics was used for modeling the kinetics of temperature field change during FSW process.

In order to determine the features of macro- and microstructure by the method of optical microscopy and of physical-mechanical properties by indentation method, welded joint microsections were made and treated by the water solution of a mixture of 5 % hydrochloric acid and 5 % orthophosphoric acid. Experimental determination of the Young's modulus by indentation was conducted to more precisely determine the data, which were used for modeling of welding. Indentation at 100 g load with automatic determination of the modulus of elasticity (E) was conducted by triangular Berkovich intenter in a computerized "Mikron-Gamma" instrument in keeping with ISO/FDIS 14577–2015; Metallic materials — Indentation test for hardness and materials parameters [12–14] (measurement of hardness value which the test allows determining, was not performed in this work). Macrostructural studies were conducted with an optical binocular (40–100 magnification), microstructural studies and navigation at indentation were performed using the instrument microscope and digital video camera for DCM500 microscopes. Investigations of the level of microstructure dispersity were conducted by scanning electron microscopy (SEM) in JSM-840 (JEOL, Japan) in secondary electron mode (SEI) at 20 kV accelerating voltage and probe current of 10^{-7} A. The electron microscope is fitted with a combined system of energy-dispersive microanalysis INCA PentaFet (INCA, England) and digital image recording system Scan Micro Capture 2.1.

In the methodology [9] of numerical analysis of the thermodeformational processes at FSW the equation of nonstationary heat conductivity is used to determine the kinetics of temperature distributions,

$$\frac{\partial}{\partial x}\left(\lambda\frac{\partial T}{\partial x}\right)+\frac{\partial}{\partial y}\left(\lambda\frac{\partial T}{\partial y}\right)+\frac{\partial}{\partial z}\left(\lambda\frac{\partial T}{\partial z}\right)+ +W(x,y,z,t)=c\rho\frac{\partial T}{\partial t}, \quad (1)$$

which allows for the power of volume heat release $W(x, y, z, t)$; ρ is the material density; c is the specific heat; λ is the coefficient of thermal conductivity; T is the material temperature (Table 2).

Boundary conditions on the joint surfaces, taking into account the convective heat exchange with the environment:

$$q = -h(T_{out} - T), \quad (2)$$

Table 2. Thermal-physical properties of MA2-1 magnesium alloy (T_m = 650 °C)

T, °C	Density, kg/m³	Young's modulus of elasticity, GPa	Yield limit, MPa	Heat conductivity coefficient λ, W/m·°C	Specific heat conductivity S, J/(cm·°C)
20	1785	42	140	1.02	1.80
100	1785	40	137	1.07	1.86
200	1761	37	134	1.12	1.92
300	1746	35	129	1.18	1.98
400	1730	32	88	1.23	2.04
500	1714	29	63	1.25	2.13

where T_{out} is the ambient temperature; q is the heat flux; h is the coefficient of heat transfer from the surface (h = 10 W/m^2·°C).

Power of heat release at FSW

$$W(x, y, z, t) = \mu P_n \omega r, \quad \text{at } z = 0,\ R1 < r < R2 \quad (3)$$

(on the upper surface in the tool shoulder zone),

at $0 < z < \delta$, $r = R1$ (across the thickness in the tool pin zone), where μ is the friction coefficient; P_n is the normal force in the contact zone; ω is the angular velocity of the tool rotation; $r = \sqrt{(x-x_0)^2 + (y-y_0)^2}$ is the distance of the contact point from the tool rotation axis (x_0, y_0); $R1$ is the pin radius; $R2$ is the shoulder radius; δ is the thickness of the plate being welded.

In the elastoplastic definition the strain tensor

$$\varepsilon_{ij} = \varepsilon_{ij}^e + \varepsilon_{ij}^p \quad (i, j = x, y, z), \quad (4)$$

where ε_{ij}^e is the tensor of elastic deformations; ε_{ij}^p is the tensor of plastic deformations. The components of tensors of stresses σ_{ij} and elastic deformations ε_{ij}^e are connected to each other by Hooke's law:

$$\varepsilon_{ij}^e = \frac{\sigma_{ij} - \delta_{ij}\sigma}{2G} + \delta_{ij}(K\sigma + \varphi) \quad (5)$$

where δ_{ij} is the unit tensor; $\sigma = \frac{1}{3}(\sigma_{xx} + \sigma_{yy} + \sigma_{zz})$, $G = \frac{E}{2(1+\nu)}$ is the shear modulus; $K = \frac{1-2\nu}{E}$ is the volumetric compression compliance; E is the Young's modulus; ν is the Poisson's ratio; φ is the function of free relative elongations (volumetric changes) caused by temperature change:

$$\varphi = \alpha(T - T_0), \quad (6)$$

where α is the coefficient of relative temperature elongation of the material.

Plastic deformations are associated with the stressed state by the equation of the theory of plastic nonisothermal flow, associated with von Mises yield condition. Iteration processes are used to solve the problem with physical nonlinearity, associated with development of plastic deformations.

The developed mathematical model allows determination of residual welding stresses and deformations in the zone of FSW butt joint, as a result of nonuniform temperature heating, because of mechanical friction of the tool against the plate material during welding. The mathematical model can be efficient for prediction of general deformations of large-sized structures with a large number of welded joints. In order to simplify the model, the following aspects were not taken into account: dependence of friction coefficient on material temperature, heating and heat removal to the work tool and fixtures.

Mathematical modeling of FSW process was conducted on 2 mm magnesium alloy plates at a constant speed of the tool rotation of 1420 rmp, and for different linear welding speeds of 8, 16, 24 m/h, using a specialized proprietary program of finite element analysis.

RESULTS

At optical examination of the macrostructure of a set of 6 samples, produced at different linear welding speeds (Figure 2), it was determined that all of them have similar and typical for FSW asymmetrical weld shape with zones of metal advancing (AS) and retreating (RS), and sound zone of intensive plastic deformation without cavities. Weld width is approximately 10 mm.

Thermodynamic processes at FSW form a clear boundary between the weld nugget and TMAZ at the retreating size (RS) (Figure 3, *a*). Basic magnesium alloy of Mg–Al system has a rolled structure with an elongated grain (Figure 3, *b*). TMAZ structure along AS has horizontal bands of metal flow diffusion from initial rotation of FSW tool with a microstructure similar to that of base metal (Figure 3, *c*). Increase of weld metal ductility from heating at torsional deformation leads to elongation and compression of metal grain boundaries, and furtheron to local extrusion and recrystallization. Here, fine round grains of 1–10 μm size are formed (Figure 3, *d* and Figure 4).

From the fundamental viewpoint, in Mg–Al chemical system, which was exposed to intensive deformation, formation of distribution phases, which consist of Mg-rich and Al-rich regions, is possible in the range of 550–640 °C. Such a temperature ensures a high mobility of the atoms, and promotes growth of the grains of dimensions from 50 up to 500 nm due to diffusion and recrystallization. At mixing of the zones with high and low temperature, this recrystallization occurs with increase of dislocation density on the grain and subgrain boundaries. So-called Lomer–

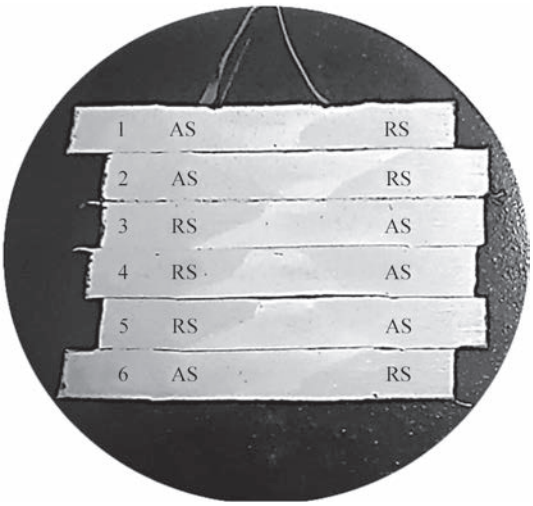

Figure 2. Macrostructure of FSW butt joints

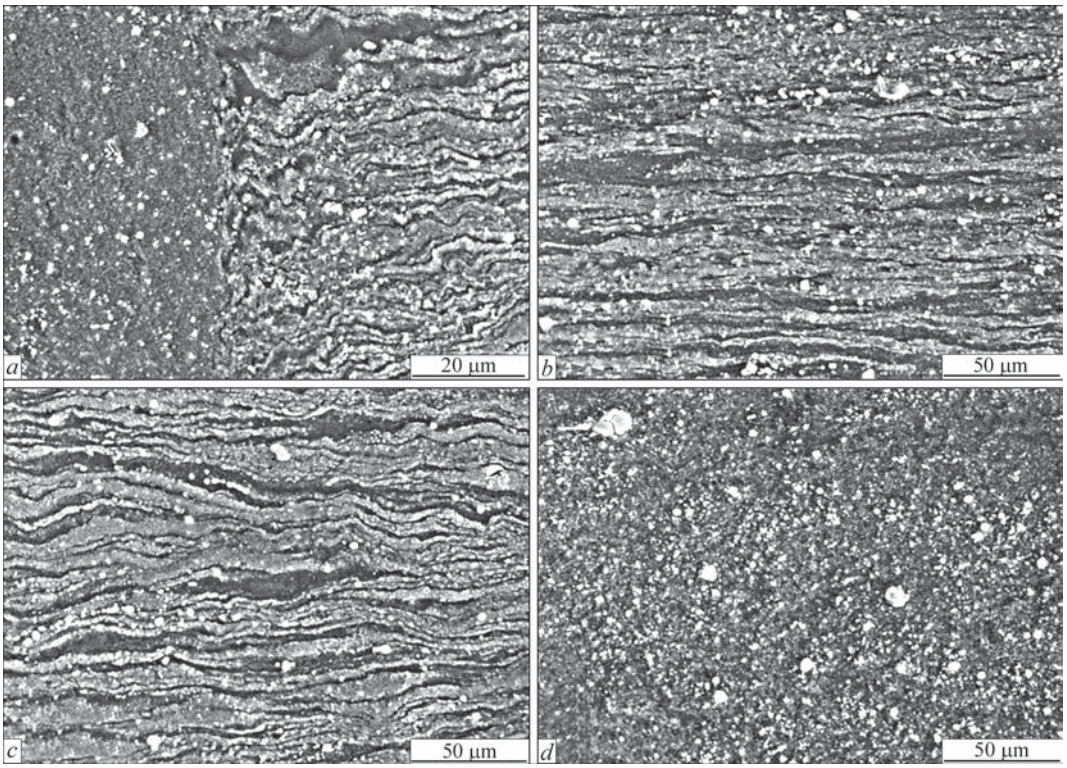

Figure 3. Microstructure of FSW weld on the retreating side (RS) – base metal (*b*), HAZ–TMAZ–weld nugget (*c*) and weld nugget middle (*d*) REM

Cottrell barriers are formed, which stop dislocation sliding because of formation of thresholds on them as a result of mutual intersection. Furtheron, they inhibit generation of new dislocations. Thus, the more difficult it is for dislocations to move in the material, the stronger is the strain hardening. Usually, formation of a fine sound structure at FSW takes place with the participation of several mechanisms simultaneously, and the result depends on the welding conditions, chemical composition of the material and other factors.

The modulus of elasticity (E) was determined for 5 types of textures of the zone of the joint — base metal, TMAZ, top, bottom and center of the nugget (Figure 5). In the nugget central part E = 30 GPa, this zone contains an ellipsoidal structure (Figure 6) and elongated from pressing and tool rotation textures in the weld upper and lower parts. For the weld upper part E = 36 GPa. The highest value E = 90 GPa was determined in the nugget at the distance of 50–150 μm along the sample lower edge. That is, elasticity is increased 2 – 3 times, compared to base metal, where E = 35 GPa. For TMAZ modulus of elasticity is E = 30 GPa.

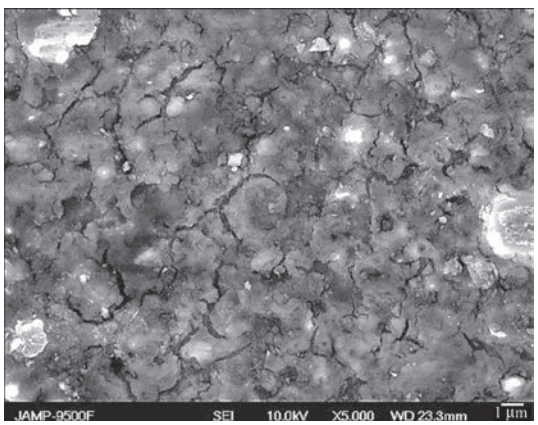

Figure 4. Fine grains in the nugget zone (SEM)

Comparison of the shape and depth of indentation diagrams shows a more ductile state of the base metal (Figure 7, *a*), and in the nugget zone below the intersection midpoint the elastic reaction of the material surface is increased (Figure 7, *b*). The depth of the indenter immersion into the base metal is greater, and it is equal to 7.57 μm, and in the nugget zone below the intersection midpoint it is equal to 5.44 μm. As such a significant inhomogeneity of the texture of FSW joint zones creates a high level of elastically deformed state in the thin metal, it ensures the traditional statistics of fracture through TMAZ at tensile strength testing. Therefore, additional heat treatment is usually recommended, after which the state can be normalized by approximately 10 % [15].

By experimental thermogram of the welding process recorded by the thermal imager, it was approximately determined that the temperature of external surface of the magnesium alloy and tool at FSW is not higher than 355.8 °C. The model of the temperature fields at the specified welding parameters (Figure 8) shows similar temperature at a small distance from the point of contact of cylindrical FSW tool with the metal, and after passing of FSW tool the temperature is at the level of 410 °C. In the zone, where a refined

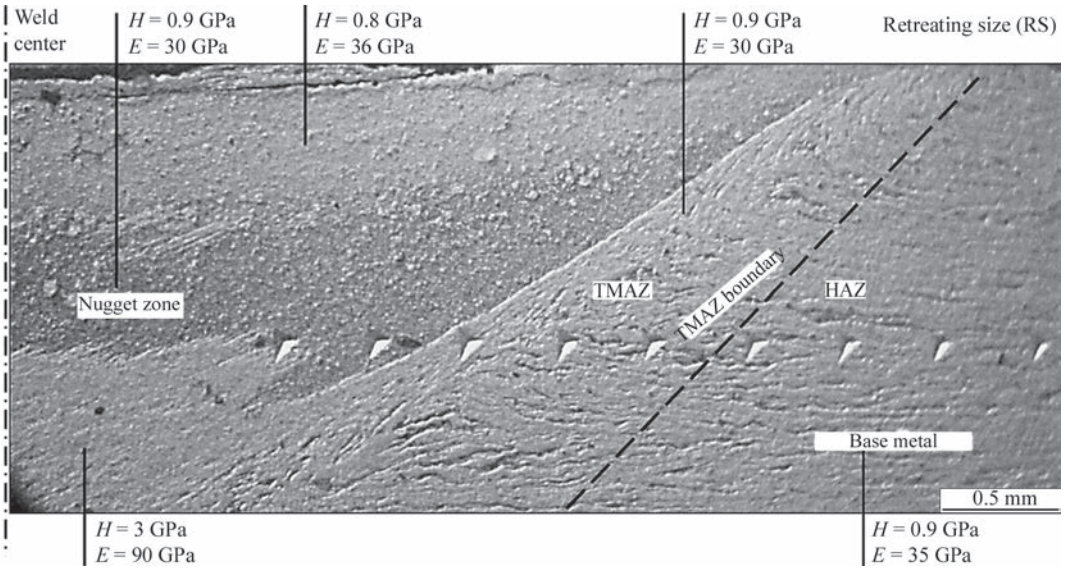

Figure 5. Distribution of hardness and Young's modulus of elasticity in FSW joint from RS

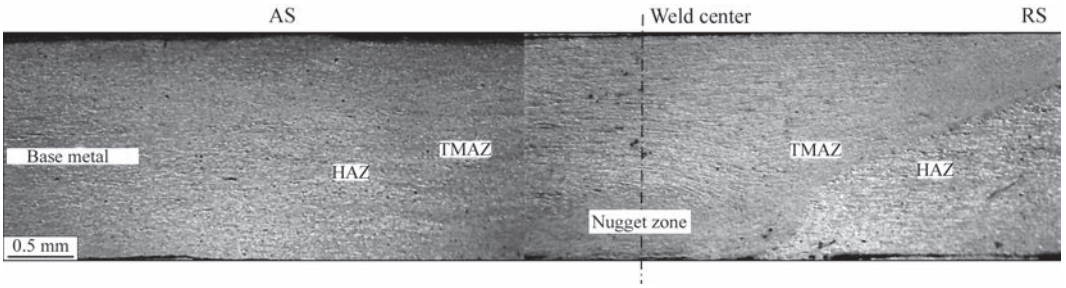

Figure 6. Microstructure of the central part of FSW with indenter imprints

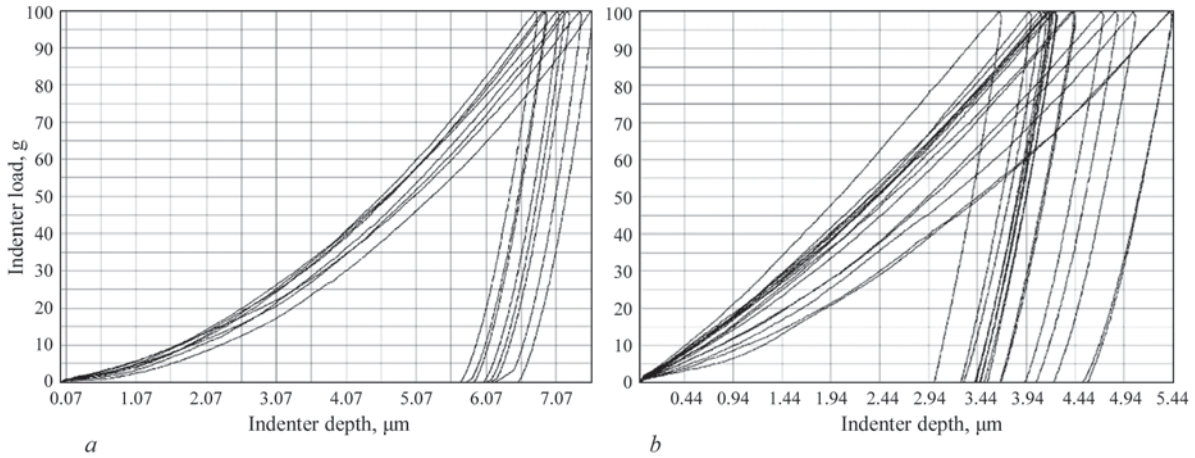

Figure 7. Diagram of indentation of base metal (*a*) and weld nugget (*b*)

structure forms with 2–3 times increase of elasticity, the temperature is equal to 500 °C.

In keeping with the thermal cycle (Figure 9, *a*), heating to the temperature of 600–610 °C, at which the welded joint forms, is not essentially dependent on linear speed of FSW tool advancing. The width of the temperature field of FSW joint zone (Figure 9, *b*) is reduced with increase of the linear speed, and it is equal to 8, 6 and 4 mm, for linear speeds of 8, 16 and 24 m/h, respectively.

The width of the weld on experimentally produced samples of FSW joints at linear welding speed of

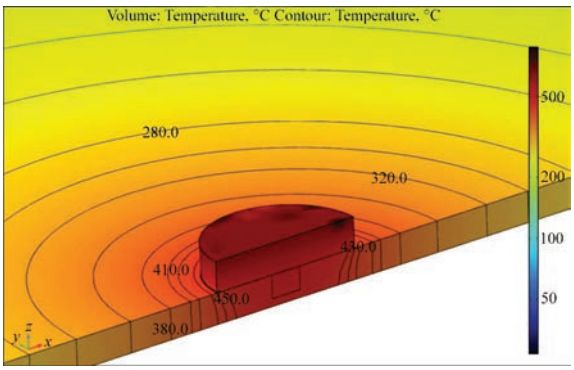

Figure 8. Model of temperature fields of FSW process

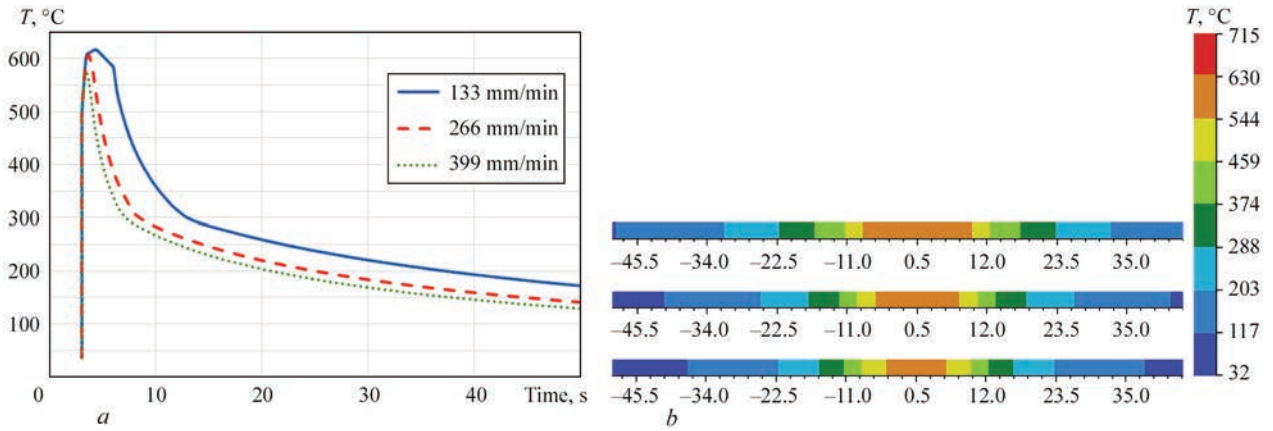

Figure 9. Distribution of thermal cycles (*a*) and temperature fields (*b*) at FSW of 2 mm plates from a magnesium alloy at different linear welding speeds

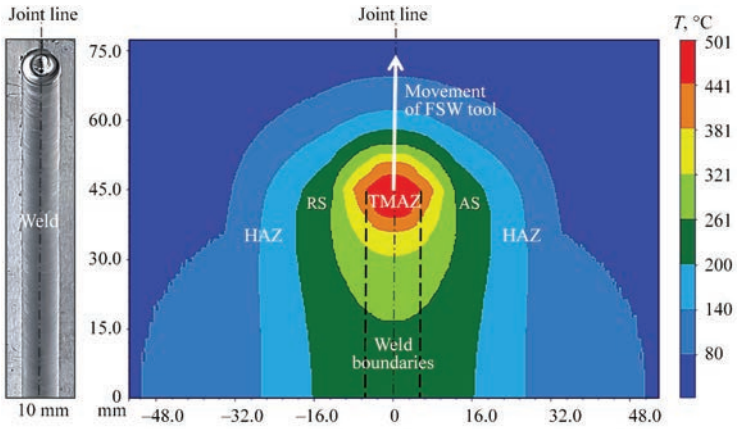

Figure 10. TMAZ width at linear speed of 8 m/h in the sample and model

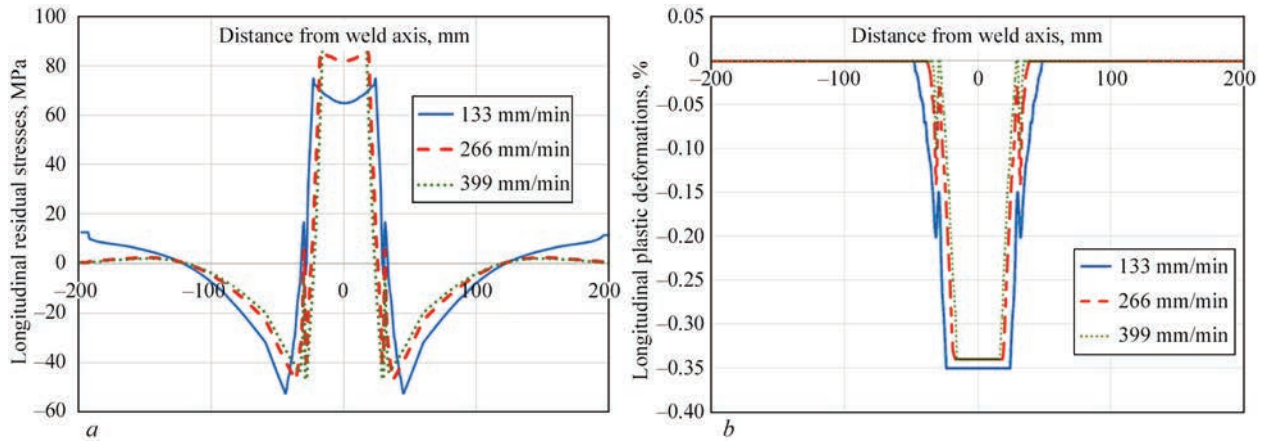

Figure 11. Distribution of longitudinal residual stresses (*a*) and plastic deformations (*b*) in the butt joint of 2 mm plates from a magnesium alloy at different FSW linear speeds

8 m/h is equal to approximately 10 mm (Figure 10) is presented in the calculation data by a similar value.

Calculations of maximal residual tensile stresses showed that they reach the material yield limit of 140 MPa (Figure 11, *a*). The level of maximal calculated residual plastic shrinkage deformations is relatively low — up to 0.35 % (Figure 11, *b*). At increase of linear welding speed, maximal residual tensile stresses increase by 10–15 %, which is related to increase of temperature gradient during welding. It was also established that residual plastic deformations (longitudinal) demonstrate a slight lowering of the level with increase of the linear welding speed.

CONCLUSIONS

Sound welded joints of thin sheets of magnesium alloy are produced at a constant frequency of FSW tool rotation of 1420 rmp and linear welding speeds of 8, 16, 24 m/h. A clearcut textured boundary between the weld nugget and TMAZ forms on the metal retreating side; weld nugget contains a refined ellipsoidal structure with 2–3 times increase of the modulus of elastic-

ity, compared to the base metal. The calculated temperature field which characterizes the FSW process, correlates with experimentally determined surface temperature and has a maximal temperature at the level of 600 °C in the nugget zone, i.e. the metal in the joint zone is in the ductile state. Modeling of the kinetics of temperature field change during FSW shows that the HAZ width decreases with increase of the linear speed. It is found that at higher linear welding speed the maximal residual stresses are increased by 10–15 %. Residual plastic deformations are decreased at increase of the linear welding speed. To produce a uniform structure of FSW weld of thin sheets of the magnesium alloy, lowering of the heat input into the metal due to increase of FSW linear speed or lowering of the speed of FSW tool rotation can be effective, i.e. it is rational to further on determine the balance of linear speed and rotation speed of FSW tool.

REFERENCES

1. Yan Yanga, Xiaoming Xionga, Jing Chen et al. (2023) Review. Research advances of magnesium and magnesium alloys worldwide in 2022. *J. of Magnesium and Alloys*, **11**, 26112654. DOI: https://doi.org/10.1016/j.jma.2023.07.011
2. Jiangfeng Song, Jing Chen, Xiaoming Xiong et al. (2022) Research advances of magnesium and magnesium alloys worldwide in 2021. *J. of Magnesium and Alloys*, 10(**4**), 863–898. DOI: https://doi.org/10.1016/j.jma.2022.04.001
3. Kostin, V.A., Falchenko, Yu.V., Puzrin, A.L., Makhnenko, A.O. (2023) Production, properties and prospects of application of modern magnesium alloys. *Suchasna Elektrometalurhiya,* **1**, 43–52. DOI: https://doi.org/10.37434/sem2023.01.06 [in Ukrainian].
4. Poklyatskyi, S.I., Motrunich, S.I., Fedorchuk, V.E., Klochkov, I.M. (2023) Strength and structure of butt, overlap and fillet joints of AMg6M alloy produced by friction stir welding. *The Paton Welding J.,* **2**, 10–17. DOI: https://doi.org/10.37434/tpwj2023.02.02
5. Krasnowski, K. et al. (2021) Relation between geometry of FSW tools and formation of nano-dispersed zones in macrostructure EN AW 6082-T6 alloy welded joints. *Biuletyn Instytutu Spawalnictwa w Gliwicach*, 65(**5**), 7–16. DOI: https://doi.org/10.17729/ebis.2021.5/1
6. Krasnovsky, K., Khokhlova, Yu.A., Khokhlov, M.A. (2019) Influence of tool shape for friction stir welding on physico-mechanical proprerties of zones of welds of aluminium alloy EN AW 6082-T6. *The Paton Welding J.,* **7**, 7–11. DOI: http://dx.doi.org/10.15407/tpwj2019.07.02
7. Tsaryk, B.R., Muzhychenko, O.F., Makhnenko, O.V. (2022) Mathematical model of determination of residual stresses and strains in friction stir welding of aluminium alloy. *The Paton Welding J.,* **9**, 33–40. DOI: https://doi.org/10.37434/tpwj2022.09.06
8. Asadi et al. (2015) Microstructural simulation of friction stir welding using a cellular automaton method: A microstructure prediction of AZ91 magnesium alloy. *Inter. J. of Mechanical and Materials Eng*. DOI: https://doi.org/10.1186/ s40712-015-0048-5
9. Makhnenko, O.V., Kandala, S.M., Basystyuk, N.R. (2021) Influence of heat transfer factor on level of residual stresses after heat treatment of reflection shield of WWER-1000 reactor. *Mech. Adv. Technol*., 5(**2**), 254–259. DOI: https://doi.org/10.20535/2521-1943.2021.5.2.245074
10. Makarenko, A.A., Makhnenko, O.V. (2022) Mathematical modeling of residual stresses in composite welded joints of WWER-1000 reactor vessel cover with CSS nozzles. *The Paton Welding J*., **1**, 33–40. DOI: https://doi.org/10.37434/tpwj2022.01.07
11. Dutka, V.A., Maistrenko, A.L., Zabolotnyi, S.D., Stepanets, A.M. (2023) Prediction of thermal state of tool from superhard materials in friction stir welding of heat-resistant alloys. *Instrumentalne Materialoznavstvo: Transact.,* Issue 26, Kyiv, ISM, 295–305 [in Ukrainian].
12. Khokhlova, Yu.A., Ishchenko, D.A., Khokhlov, M.A. (2017) Indentation from macro- to nanometer level and examples of investigation of properties of materials with a special structure. *Tekh. Diahnost. ta Neruiniv. Kontrol,* **1**, 30–36. DOI: https://doi.org/10.15407/tdnk2017.01.05 [in Ukrainian].
13. Oliver, W.C., Pharr, G.M. (1992) An improved technique for determining the hardness and elastic modulus using load displacement sensing indentation experiments. *J. Mater. Res*., **7**, 1564–1583. DOI: https://doi.org/10.1557/JMR.1992.1564
14. Kazuhisa Miyoshi (2002) NASA/TM-2002-211497: *Surface characterization techniques: An overview*. 12–22. http://ntrs.nasa.gov/archive/nasa/casi.ntrs. nasa.gov/20020070606.pdf
15. Kulwant Singh, Gurbhinder Singh, Harmeet Singh (2019) Microstructure and mechanical behaviour of friction-stir-welded magnesium alloys: As-welded and post weld heat treated, 20, September 100600. DOI: https://doi.org/10.1016/j.mtcomm.2019.100600

ORCID

M.A. Khokhlov: 0000-0002-8180-3459,
V.A. Kostin: 0000-0002-2677-4667,
A.G. Pokliatskyi: 0000-0002-4101-2206,
Iu.V. Falchenko: 0000-0002-3028-2964,
Yu.A. Khokhlova: 0000-0002-2145-973X

CONFLICT OF INTEREST

The Authors declare no conflict of interest

CORRESPONDING AUTHOR

Yu.A. Khokhlova
E.O. Paton Electric Welding Institute of the NASU
11 Kazymyr Malevych Str., 03150, Kyiv, Ukraine.
E-mail: khokhlova.julia@gmail.com

SUGGESTED CITATION

M.A. Khokhlov, O.O. Makhnenko, V.A. Kostin, A.G. Pokliatskyi, Iu.V. Falchenko, Yu.A. Khokhlova (2024) Thermomechanical processes in friction stir welding of magnesium alloy sheets. *The Paton Welding J*., **5**, 11–17.

JOURNAL HOME PAGE

https://patonpublishinghouse.com/eng/journals/tpwj

Received: 07.03.2024
Received in revised form: 16.04.2024
Accepted: 31.05.2024